Surface barrier in W(110). II. Low-energy electron diffraction fine-structure analysis

P. J. Jennings
School of Mathematical and Physical Sciences, Murdoch University, Murdoch W A 6150, Australia

R. O. Jones
Institut für Festkörperforschung der Kernforschungsanlage Jülich, Postfach 1913, D-5170 Jülich, Federal Republic of Germany

(Received 27 June 1986)

High-resolution experimental data for the low-energy electron diffraction fine structure in W(110) are analyzed using a one-dimensional model potential barrier used previously for W(001). The measured fine structure is reproduced very well for both surfaces, and the optimum barriers are similar. The position of the image plane in W(110), however, is approximately 0.2—0.3 a.u. farther from the outermost layer of atoms than in W(001). This is in good agreement with the results of self-consistent electronic-structure calculations reported by Jepsen and Jones in the preceding paper.

I. INTRODUCTION

The last decade has seen continuing improvement in experimental techniques for studying surfaces, an example being the high resolution obtained in low-energy diffraction (LEED) measurements.[1] The fine structure observed at low energies provides us with the most sensitive test presently available of the details of the scattering potential for electrons at surfaces. The "surface barrier" problem, particularly for metal surfaces, has been of interest for many years. Among many simple models proposed[2] was one based on self-consistent electronic-structure calculations for a five-layer W(001) film:[2]

$$V(z)=\begin{cases}\{1-\exp[\lambda(z-z_0)]\}/[2(z-z_0)], & z<z_0\\ -U_0/\{A\exp[-B(z-z_0)]+1\}, & z>z_0\,.\end{cases} \quad (1)$$

A and B are determined by matching $V(z)$ and its normal derivative at $z=z_0$ ($A=-1+2U_0/\lambda$, $B=U_0/A$). The parameters which enter are the position of the image plane z_0, the bulk inner potential U_0, and λ, which determines the range of transition between the vacuum and bulk potentials. The value of the potential at $z=z_0$ is $-\lambda/2$. Small values of λ produce a strongly saturated barrier, while larger values lead to one closely resembling the modified image barrier[2] used in earlier work. Negative values of A lead to barriers with an unphysical form, so that λ cannot be larger than $2U_0$. Since the electronic-structure calculations for W(001) suggest a value of $\lambda\sim U_0$, the barrier height at the image plane should be about half of the inner potential.

The image plane position remains the subject of much interest. It determines not only the interaction potential of an electron far from the surface,

$$V(z)=1/[2(z-z_0)]\,, \quad (2)$$

but gives the center of mass of the surface charge density induced by a weak uniform electrostatic field outside the surface. The dynamic image-plane position for time-dependent external fields determines the van der Waals interaction between an atom and a metal surface.[3] Results of calculations[4–6] of the static image-plane position (z_J, relative to the edge of the positive background) are shown in Table I for the jellium model of a metal surface for different bulk electron densities. In this model, the image plane lies outside the edge of the uniform positive background. If the latter can be associated with the plane midway between two atomic layers, values of z_0 relative to this plane should lie in the range 2.5—3.5 a.u. for most metal surfaces.

The improvement in experimental resolution has meant that discrimination between different models as descriptions of real surfaces is becoming possible. In the case of W(001), our previous work[1,2] showed that a barrier of the form (1) with (z_0,λ) values in a narrow valley between (2.6,1.1) and (3.3,0.7) could reproduce measured features in high-resolution LEED data very well, with an optimum barrier near (2.9,0.9). This value of z_0 is very close to that found from fitting the results of the film calculations for the same surface. It is natural to ask whether the same model barrier can be applied to other materials and to other faces of tungsten.

The measured anisotropies in work function and inner potential show that different crystal surfaces have different potential distributions. The work functions Φ of the (110), (100), and (111) surfaces of tungsten, for example, are 5.25, 4.63, and 4.47 eV,[7] respectively, i.e., Φ decreases with decreasing density of surface atoms. The inner potential U_0 is approximately 1 eV greater for W(110) than for W(001).[8] A comparison of LEED fine-structure calculations with experiment was performed recently for W(001) and W(110) by Baribeau *et al.*[9] The model barrier they used was similar to (1), but with the

TABLE I. Distance of image plane from jellium background, z_J, for different values of r_s.

r_s	Ref. 4	Ref. 5	Ref. 6
2	1.61	1.61	1.57
3		1.42	1.35
4	1.30	1.23	1.25

inner potential in the outermost atomic layer different from the bulk value. They concluded that the difference is nearly 4 eV in W(001), but only 0.5 eV in W(110). Furthermore, the location of the image plane, z_0, was predicted to be significantly closer to the surface in W(110) ($z_0=-2.72$ a.u.) than in W(001) ($z_0=-3.67$ a.u.).

In the preceding paper, Jepsen and Jones[10] described the results of self-consistent electronic-structure calculations of the W(110) surface and compared the form of the potential distribution with earlier results for W(001).[1] This comparison showed that the larger inner potential on the more densely packed W(110) surface was associated with a barrier origin, z_0, approximately 0.3 a.u. *farther* from the surface than in W(001), i.e., a trend opposite to that predicted by Baribeau *et al.*[9] In the present work, we analyze high-resolution LEED data on W(110) using a model barrier of the form (1). In Sec. II we outline the method used and compare calculated intensity curves with experiment, and in Sec. III we discuss the results and the consequences both of this work and the electronic-structure calculations of the preceding paper.[10] Our concluding remarks are contained in Sec. IV.

II. METHOD OF CALCULATION AND APPLICATION TO W(110)

The method used to analyze LEED fine-structure data has been described in detail elsewhere.[1,2] The geometry of the surface is assumed to be the same as in the bulk, i.e., as shown in Fig. 1(a) of the preceding paper,[10] and the scattering potential for electrons to have muffin-tin form. The (energy-dependent) bulk and surface damping parameters have the forms used previously for W(001). In general, the remaining parameters U_0, z_0, and λ are also energy-dependent and, in the case of U_0, this can be found from the positions of the Bragg peaks. The connection between $U_0(z_0)$ and λ noted above implies a related energy dependence of $\lambda(E)$. In the analysis of W(001) (Ref. 2) and in the present work we have assumed

$$\lambda(E)=U_0(E)\lambda(0)/U_0(0)\ . \tag{3}$$

The first step in the analysis is then to determine $U_0(E)$, followed by the optimization of the parameters $\lambda(0)$ and z_0. We have performed an extensive series of calculations without relativistic effects, and refined the barrier using a fully relativistic program.[11] Our earlier calculations on W(001) showed that some features present in non-spin-polarized measurements can be traced unambiguously to the effects of spin and cannot be reproduced by calculations which neglect them. The calculations of W(001) and the present work on W(110) show, however, that the spin dependence of the fine-structure peak positions is small.

The data base for the present study is taken from the work of Baribeau, Carette, and co-workers[9,12,13] for the specular (00) beam. This beam is the most suitable for fine-structure analysis, since its position remains fixed for a constant angle of incidence, and it is observable for all energies in the range 0–20 eV, where the most pronounced fine structure occurs. In the [11] azimuth,[14] the fine structure associated with the $(\bar{1}\,\bar{1})$ emergence occurs near 8 eV, and for the $(\bar{1}0)$ and $(0\bar{1})$ beams, near 15 eV. The $[\bar{1}1]$ azimuth has emergences near 9 eV $[(10),(0\bar{1})]$ and 15 eV $[(1\bar{1})]$, and the [01] azimuthal plane, an emergence near 6 eV $[(0\bar{1})]$. The emergence of degenerate beams leads to very weak oscillations in all cases. We study here the remaining thresholds, for $[\bar{1}1]$ with $\theta=70°,80°$; [01] with $\theta=60°,70°$, and [11] with $\theta=45°,60°,75°$. The Bragg-peak positions show that U_0 is close to 15 eV at incident energy E near zero, falling to 14 eV near $E=10$ eV and to 13.5 eV for $E\sim 20$ eV. The low-energy value is similar to that found in other work,[8] and the variation with energy very similar to that found in Cu(001),[15] Ni(001),[15] and W(001).[2] The energy dependence of λ [Eq. (3)] was determined from this behavior.

As noted above, an extensive optimization of the parameters z_0,λ was performed using a nonrelativistic program.[16] The results show two features which we and others have noted in earlier work.[1,2,9] (i) For each incident condition (θ,ϕ) there is a narrow valley in z_0,λ space where the model barrier reproduces the experimental data well. Moving the barrier farther from the surface (increasing $|z_0|$) while increasing the range of transition from vacuum to bulk (decreasing λ) results in barriers with qualitatively similar shapes and scattering properties. However, the valley has steep sides. If we increase both λ and $|z_0|$, for example, there are dramatic changes in the calculated fine structure. (ii) For a given azimuth the optimum value of λ increases slightly with increasing θ. This was also apparent for W(001) and, while it may be evidence for a velocity-dependent or three-dimensional ef-

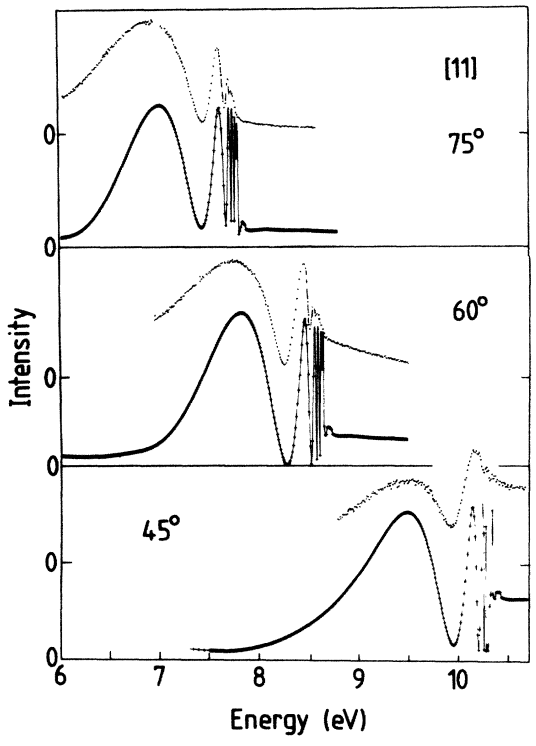

FIG. 1. Comparison of calculated (connected crosses, $z_0=-3.0$, $\lambda=0.85$, energy mesh 0.01 eV) and experimental (points) fine structure for W(110) for the [11] azimuth.

fect,[1] it is small and may reflect no more than a systematic experimental uncertainty. It is important to note that the interference origin of the fine structure means that several distinct regions of z_0,λ space exist for which satisfactory agreement with experiment can be obtained.[11]

The barrier was refined in the region with z_0 values similar both to those found for the W(001) surface and in electronic-structure calculations for W(110) (Ref. 10) ($2.6 \leq |z_0| \leq 3.5$ and $0.7 \leq \lambda \leq 1.0$). We used the relativistic method described earlier,[1,2,11] with a fine mesh for the barrier parameters ($\Delta z_0 = 0.05$, $\Delta\lambda = 0.05$) and an energy mesh of 0.01 eV. The data were for the incident conditions given above. With one exception ([11] azimuth, $\theta = 45°$), at least four (usually six to eight) maxima and minima are resolved clearly for each curve. In the present analysis, we focus on the relative *positions* of these extrema, and have adjusted the experimental energy scales by a small amount (≤ 0.1 eV) so that the last well-resolved maximum prior to threshold coincides with the calculated peak. Our optimization procedure does not use the relative *intensities* of the peaks. These are affected most by changes in the damping parameters, and these are fixed in the present calculations.

III. RESULTS AND DISCUSSION

In Figs. 1–3 we compare the measured fine structure with calculations for a non-spin-polarized incident electron beam using the optimum barrier parameters for each set of incident conditions. As in the case of W(001), we find in each case a narrow valley in z_0,λ space for which satisfactory agreement can be found. In the case of the [$\bar{1}$1] azimuth, for example, the results with barrier parameters $-3.1, 0.9$ and $-3.2, 0.85$ are virtually indistinguishable. The comparison is shown for parameters near the center of each valley. It is apparent that a very good fit to the experimental fine structure can be found in all cases.

The values of z_0 and λ which give the best fits to the experimental data depend only weakly on incident and azimuthal angles. For fixed ϕ, there is a tendency for λ to increase with increasing θ. Although the beam giving rise to the fine structure in the [$\bar{1}$1] azimuth emerges at higher energies (15–18 eV) than for the other incident conditions discussed here, the value of $\lambda(0)$ is not significantly different. The assumed energy dependence of λ [Eq. (3)] means that the actual value of λ is smaller. The results for the [11] azimuth give an optimum z_0 value slightly closer to the surface. In fact, a barrier with parameters $z_0 = 3.1$ a.u. and $\lambda = 0.90$ a.u.$^{-1}$ reproduces the experimentally resolved fine structure very well, i.e., it can describe the relative positions of the intensity maxima and minima with an accuracy close to the resolution of the apparatus. The latter depends, of course, on the width of the extremum.[13]

The barrier parameters found for W(110) are remarkably similar to those for W(001), and the two barriers are shown in Fig. 4. Apart from the difference in the inner potential, the main difference is the position of the image plane, which is farther from the outermost atomic layer in W(110). In spite of the uncertainty in the determination of the barrier parameters, this is a significant difference.

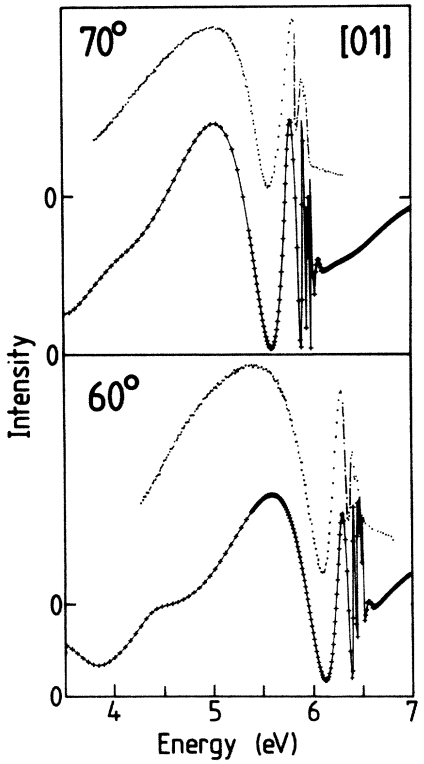

FIG. 2. Comparison of calculated (connected crosses, $z_0 = -3.1$, $\lambda = 0.9$, energy mesh 0.01 eV) and experimental (points) fine structure for W(110) for the [01] azimuth.

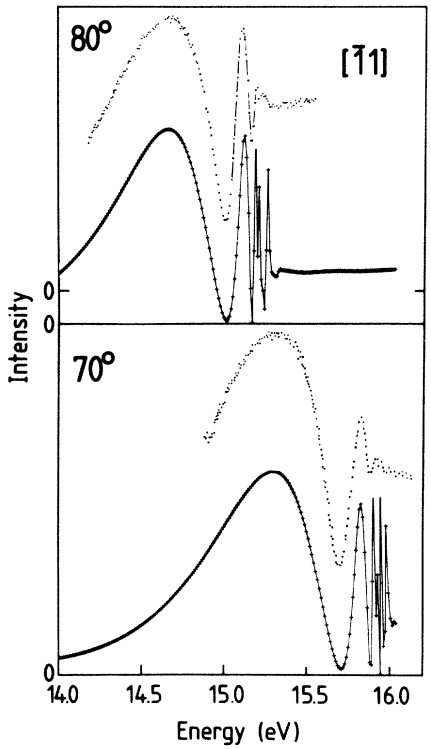

FIG. 3. Comparison of calculated (connected crosses, $z_0 = -3.1$, $\lambda = 0.9$, energy mesh 0.01 eV) and experimental (points) fine structure for W(110) for the [$\bar{1}$1] azimuth.

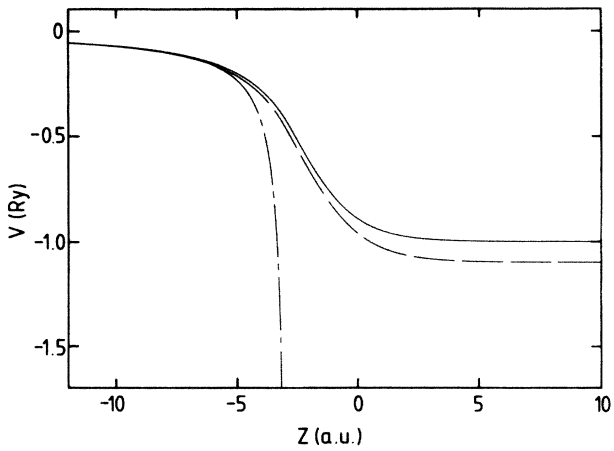

FIG. 4. One-dimensional barrier models. Chain curve: image potential with $z_0=-2.9$ a.u.; solid curve: W(001) with $z_0=-2.9$ a.u., $\lambda=0.9$ a.u.$^{-1}$, $U_0=1.0$ Ry; dashed curve: W(110) with $z_0=-3.1$ a.u., $\lambda=0.9$ a.u.$^{-1}$, $U_0=1.1$ Ry.

The same method for comparing theory and experiment was used for both surfaces, and the narrow valleys in z_0,λ space leading to a very good fit are translated almost rigidly by ~ 0.3 a.u. It is satisfying that the magnitude and sign of the difference is consistent with the results of the electronic-structure calculations for the two faces. We believe that electronic-structure and high-resolution LEED calculations provide complementary information essential to an understanding of the potential barrier at metal surfaces.

As noted above, Baribeau *et al.*[9] have also performed a barrier analysis on W(001) and W(110). For the latter, the data base included the first four maxima and minima for $\theta=50°$, 65°, and 80° along the [11] azimuth, and $\theta=85°$ along the $[\bar{1}1]$ azimuth. They were able to reproduce the experimental fine structure very well. Apart from the absence of relativistic effects in their calculations, an essential difference between their work and ours is that they allowed the outermost atomic layer to have a different muffin-tin zero, V_s, from that in the bulk. The film calculations in Ref. 10 suggest that the outermost atomic layer in W(001) has a less attractive potential than in the bulk, but the difference between the two surfaces is less than 4 eV for electrons below the Fermi energy. Baribeau *et al.* found that the image plane in W(110) lies substantially closer to the outermost atomic layer than in W(001), and present arguments why this should be so. The density-functional calculations show, however, that the reverse should be true.

IV. CONCLUDING REMARKS

The comparison of calculated and measured high-resolution LEED fine structure performed here has shown that, with reasonable parameters for the bulk and surface damping, the fine structure can be reproduced very well using one-dimensional barriers with a small range of parameters near $z_0=3.1$ a.u. and $\lambda=0.9$ a.u.$^{-1}$ The optimum barrier is only weakly dependent on incident and azimuthal angles in the range considered.

The weak dependence of the optimum one-dimensional barrier on incident conditions indicates that velocity-dependent, three-dimensional, and thermal effects are less important to fine-structure studies than the overall barrier shape. However, the absence of unambiguous evidence for these effects does not imply that they are negligible. The electronic-structure calculations for both W(001) and W(110) show pronounced non-muffin-tin contributions to the effective potential experienced by electrons below the Fermi energy, and similar effects will certainly occur for incident low-energy electrons.

These calculations complete a set of parallel LEED and self-consistent electronic-structure calculations on W(001) and W(110). The results of the W(001) electronic-structure calculations were the basis for the barrier model we have adopted [Eq. (1)], and it is encouraging that the difference between the image planes for the two surfaces determined for the two surfaces in the electronic-structure calculations has the same sign and magnitude as determined by LEED. In view of the ambiguities inherent in the study of any interference phenomenon, we believe that the electronic-structure calculations complement the electron scattering work in an essential way.

The improvement in resolution in LEED measurements in recent years has meant a continuing refinement of surface barrier models. The model used here is based on the results of detailed electronic-structure calculations, and is capable of further refinement by introducing three-dimensional components (e.g., of the form found in the present film calculations) or a layer-dependent inner potential.[9] It is important to note, however, that it is impracticable to adjust all of the parameters describing the scattering potential. Some potential terms; in particular, those describing inelastic processes, have not been optimized in the present work. Damping effects are most clearly evident in the absolute reflectivities, for which relatively few data are available. Accurate estimates of absolute intensities would then be a valuable aid in discriminating between different barrier models. Furthermore, it has been shown by Gaubert *et al.*[17] that the ability to resolve fine structure depends strongly on the propagation direction of the preemergent beam relative to the plane of incidence, so that the effective experimental resolution may be substantially less than the nominal energy resolution of the apparatus.

Although the electronic-structure and LEED calculations result in a consistent picture of the surface barriers in W(001) and W(110), the detailed study of other effects remains open. This will require more very-high-resolution data on these and other surfaces. The acquisition of such data remains a difficult challenge to the experimentalist, and its interpretation will require thorough analysis using a correspondingly fine energy mesh.

ACKNOWLEDGMENT

We thank J.-M. Baribeau and the late J.-D. Carette for providing original data and copies of work prior to publication.

[1]See, for example, J.-M. Baribeau, J.-D. Carette, P. J. Jennings, and R. O. Jones, Phys. Rev. B **32**, 6131 (1985), and references therein.
[2]R. O. Jones, P. J. Jennings, and O. Jepsen, Phys. Rev. B **29**, 6474 (1984). This paper contains a survey of barrier models.
[3]See, for example, A. Liebsch, Phys. Rev. B **33**, 7429 (1986), and references therein.
[4]N. D. Lang and W. Kohn, Phys. Rev. B **7**, 3541 (1973).
[5]W. Schmickler and D. Henderson, Phys. Rev. B **30**, 3081 (1984).
[6]A. Liebsch, Phys. Rev. B **32**, 6255 (1985).
[7]R. W. Strayer, W. Mackie, and L. W. Swanson, Surf. Sci. **34**, 225 (1973).
[8]H. J. Herlt, R. Feder, G. Meister, and E. G. Bauer, Solid State Commun. **38**, 973 (1981).
[9]J.-M. Baribeau, J. Lopez, and J.-C. Le Bosse, J. Phys. C **18**, 3083 (1985).
[10]O. Jepsen and R. O. Jones, preceding paper, Phys. Rev. B **34**, 6695 (1986).
[11]R. O. Jones and P. J. Jennings, Phys. Rev. B **27**, 4702 (1983). See also P. J. Jennings and R. O. Jones, Solid State Commun. **44**, 17 (1982).
[12]J.-M. Baribeau and J.-D. Carette, Phys. Rev. B **23**, 6201 (1981); Surf. Sci. **112**, 241 (1981).
[13]J.-M. Baribeau and D. Roy, Surf. Sci. **166**, 234 (1986).
[14]Azimuths are defined using the reciprocal-lattice vectors defined in Fig. 1 of Ref. 10. This is the same convention as adopted in Ref. 9.
[15]P. J. Jennings and S. M. Thurgate, Surf. Sci. **104**, L210 (1981).
[16]Preliminary results are given in P. J. Jennings and R. O. Jones, Appl. Surf. Sci. **22/23**, 35 (1985).
[17]C. Gaubert, R. Baudoing, Y. Gauthier, and J. Rundgren, Surf. Sci. **147**, 162 (1985).